

## Quenching experiments on various thermal properties under saturated and subcooled water condition with high-speed visualization

Tong Kyun Kim<sup>a</sup>, Jun – young Kang<sup>b</sup>, Gi Cheol Lee<sup>c</sup>, Hyunwoo Noh<sup>c</sup>, Moo Hwan Kim<sup>a,c</sup>, Hyun Sun Park<sup>a\*</sup>

<sup>a</sup>Division of Advanced Nuclear Engineering, POSTECH, 77 Cheongam-Ro. Nam-Gu. Pohang. Gyeongbuk. Korea, 37673

<sup>b</sup>Thermal-Hydraulic Safety Research Division, Korea Atomic Energy Research Institute, Daejeon, 34057, Republic of Korea

<sup>c</sup>Department of Mechanical Engineering, POSTECH, 77 Cheongam-Ro. Nam-Gu. Pohang. Gyeongbuk. Korea, 37673

\*Corresponding author: hejsunny@postech.ac.kr

### 1. Introduction

The Fukushima Daiichi nuclear disaster resulted from the failure of Emergency Core Cooling System (ECCS), which caused loss-of-coolant-accident (LOCA). The amount of Hydrogen from the cladding reached the explosive concentration limit, exploding afterwards [1,2]. After the disaster, nuclear safety groups undertook research and developed an accident tolerant fuel-cladding (ATF) [4].

Oxidation resistance is an important property of ATF that can prevent hydrogen generation [5]. Many ATFs, including FeCrAl, SiC and ZrSi<sub>2</sub>, were developed due to their excellent oxidation resistance. Oxidation resistance and mechanical strength tests have been main focus of ATF [5, 6]. In respect of research on heat transfer properties, critical heat flux (CHF), which is safety margin, has been estimated to operate light water reactor (LWR) [7]. Since prediction of LOCA requires an accurate calculation of core cooling heat transfer in order to apply ATF to LOCA, post-CHF regime should be evaluated under saturated and subcooled condition.

In this study, the objective was to evaluate post-CHF regime of ATF with subcooled effect for its application to LOCA. Quenching tests were conducted for ATF candidate materials, SiC and FeCrAl, to evaluate post-CHF parameter (minimum film boiling temperature  $T_{MFB}$ , minimum heat flux  $q''_{min}$  and heat transfer coefficient in film boiling  $h_{film}$ ) under saturated and subcooled water condition. Vapor motion was visualized by high-speed camera to evaluate post-CHF parameter.

### 2. Experiment

#### 2.1 Experiment setup and specimens

Fig 1 shows the equipment for the experiment and the test specimens. Test specimens were SiC (Energyn Inc), FeCrAl (71Fe-21Cr-5Al-5Mo alloy, APMT Kanthal) and Zircaloy-4 (Alloy Zry4, UNS R60804). SiC was fabricated under pressureless-sinter, and 60

um thick SiC was deposited on the sintered body by chemical vapor deposition. The shape of test specimens was cylinder rod (diameter 10 mm and height 60 mm). The specimen temperature was measured by a thermocouple which was sheathed by Inconel (Diameter 0.5mm, K-type, OMEGA) at the center. In order to reduce thermal resistance between the thermocouple and the test specimens, thermal grease (Arctic cooling, MX-4) was used. SUS316L tube was employed to protect thermocouple from thermal damage. Quenching pool contained 4L of distilled water as working fluid and had 0.5 kW immersion heater. 1.2 kW radiation furnace was utilized to heat test specimens. The furnace and immersion heater temperature were controlled by proportional integral derivative (PID) system. The test specimens were transported by rod-less cylinder, and reflux condenser maintained water level by condensing steam. Temperature data of test specimens was collected by data acquisition system (National Instrument). Thickness and wavy motion of vapor film were visualized by high-speed camera (Vision research, phantom Miro). The test specimens were heated up to 800 °C and quenched under atmosphere pressure at 80 °C and 97 °C of DI water condition.

By measuring the temperature of the test specimens, cooling curves were obtained (Fig 2). Since Biot number of Zircaloy4, FeCrAl and SiC were 0.05, 0.05

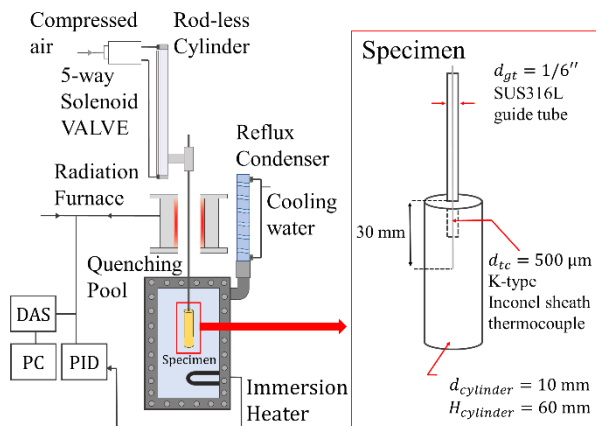


Fig. 1. Experiment equipment and test specimen

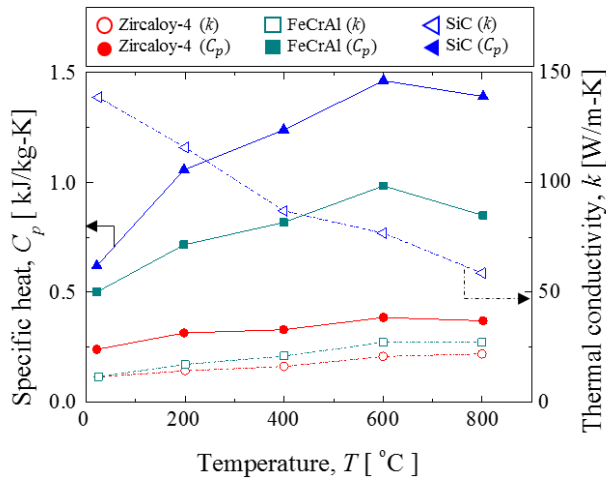


Fig. 2. Specific heat and thermal conductivity of Zircaloy-4, FeCrAl and SiC depend on temperature

and 0.02, respectively, lumped parameter method can be used to calculate heat flux,  $q''$  using Eq. (1).

$$q'' = \frac{\rho C_p V}{A} dT/dt \quad (1)$$

Thermal properties (Density  $\rho$ , specific heat  $C_p$  and thermal conductivity  $k$ ) were measured by the Korea Institute of Ceramic Engineering and Technology (KICET). Density of Zircaloy-4, FeCrAl and SiC were 6.13, 6.98 and 3.13 g/cm<sup>3</sup>, respectively. Specific heat capacity and thermal conductivity were varied from temperature (Fig 2). Volume (V) and area (A) of specimen were 4.71 cm<sup>3</sup> and 20.41 cm<sup>2</sup>.  $dT/dt$  was measured from cooling curve in film boiling regime (Fig 3). Surface characteristic of specimens was estimated with roughness (AFM, Atomic force microscope; VECO Dimension 3100 ver 7.0) and contact angle (Femtofab; Smartdrop).

## 2.2 Cooling performance

ATF material specimens, FeCrAl, SiC and Zircaloy-4 for comparison, were quenched under saturated (97 °C) and subcooled (80 °C) condition. Cooling curves were obtained as Fig 3. Under saturated condition, the entire quenching time of Zircaloy-4, SiC and FeCrAl were 29, 50 and ~90 s, respectively. Under subcooled condition, that of Zircaloy-4, SiC and FeCrAl were 19, 28 and 39 s, respectively. The entire quenching time of subcooled condition was shorter than that of saturated condition for each Zircaloy-4, FeCrAl and SiC. Heat capacity  $\rho V C_p$  of Zircaloy-4, SiC and FeCrAl were 7.00, 9.05 and 16.60 J/K at 25 °C, respectively. Even though specific heat depended on temperature, trends of the specific heat among specimens did not change (Fig 2). The entire

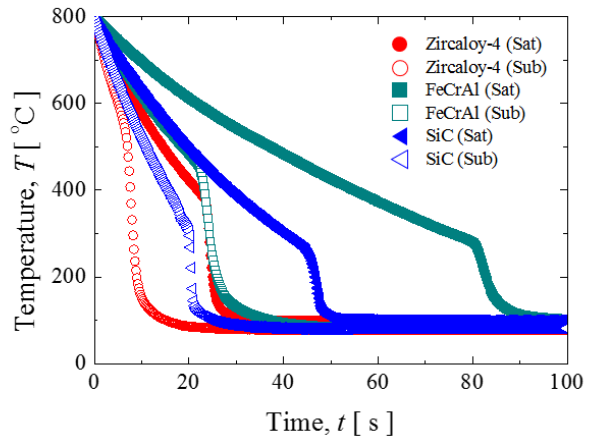


Fig. 3. The cooling curves of Zircaloy-4, FeCrAl and SiC under saturated and subcooled condition

quenching time increased as heat capacity increased in both of the saturated and subcooled condition. The entire quenching time seemed to depend on heat capacity.

The reason for the difference of quenching time between saturated and subcooled condition was the difference in vapor film thickness surrounded by specimens. In film boiling, specimens are surrounded by vapor and heat travels through vapor film due to conduction [8]. Since the vapor film works as thermal resistance, thick vapor film leads to low film boiling heat transfer coefficient [8]. The vapor film thickness  $\delta$  of ATF under saturated and subcooled condition were measured as in Fig 5. The thickness of vapor film of Zircaloy-4, FeCrAl and SiC under saturated condition were 0.9, 0.6 and 0.8 mm, respectively. That of ATF under subcooled condition was 0.3 mm. The vapor film under saturated condition had larger wavy motion than subcooled condition. Since the vapor film in subcooled condition was thinner than in saturated condition, subcooled condition led to fast cooling time (Fig 4).

## 2.3 Post-CHF parameter

Fig 5 is heat flux verse wall superheat graph. Wall superheat,  $\Delta T$  is the difference between wall temperature of specimens and surrounding temperature,  $T_\infty$ . Since Biot number of specimens was less than 0.1, heat flux was calculated from lumped method (Eq. (1)) and center temperature of specimens represent wall temperature of specimens. Minimum film boiling temperature was measured when heat flux curves of specimens had minimum heat flux in Fig 4. Minimum heat flux of Zircaloy-4, SiC and FeCrAl were 61, 58 and 66 kW/m<sup>2</sup>, respectively under the saturated condition. Minimum film boiling temperature of Zircaloy-4, FeCrAl and

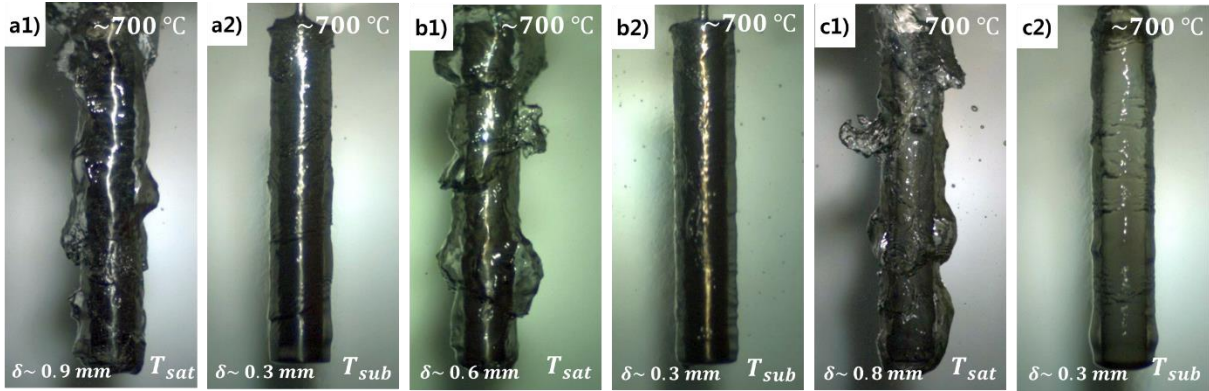


Fig. 4. Image of ATF quenching at 700 °C under saturated and subcooled condition a) Zircaloy-4, b) FeCrAl and c) SiC

SiC were 385, 283 and 268 °C, respectively under the saturated condition. Minimum heat flux of Zircaloy-4, SiC and FeCrAl were 164, 185 and 177 kW/m<sup>2</sup>, respectively under the subcooled condition. Minimum film boiling temperature of Zircaloy-4, FeCrAl and SiC were 609, 507 and 364 °C, respectively under the subcooled condition. Film boiling heat transfer coefficient of Zircaloy-4, FeCrAl and SiC could be calculated by  $h_{film} = q''_{min}/(T_{min} - T_{\infty})$ .

Minimum film boiling temperature under the saturated condition could be calculated by Henry and Berenson equation (Eq. (2) and Eq. (3)) [9, 10].  $h_{iv}$ ,  $s$ ,  $l$ ,  $v$ ,  $\sigma$ ,  $g$  and  $\mu$  indicate the latent heat of vaporization, specimen, liquid, vapor, surface tension, gravity acceleration and dynamic viscosity,

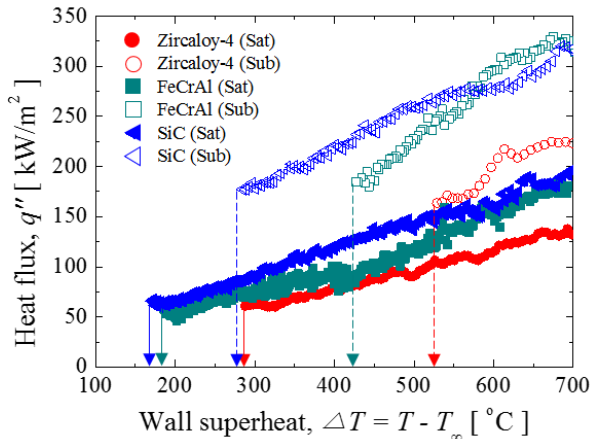


Fig. 5. Heat flux curves of Zircaloy-4, FeCrAl and SiC under saturated and subcooled condition

Property	Value		
	Zircaloy-4	FeCrAl	SiC
Roughness (μm)	0.54	0.22	1.94
Contact angle (°)	64±5	82±4	41±5

Table 1. Surface characteristic of Zircaloy-4, FeCrAl and SiC

respectively. Minimum film boiling temperature of Zircaloy-4, FeCrAl and SiC under the saturated condition from Henry equation were 446, 300 and 246 °C, respectively. That of Zircaloy-4, FeCrAl and SiC under the subcooled condition from Henry were 506, 326 and 257 °C, respectively. The difference between experimental data and Henry equation under the saturated condition was 61 °C for Zircaloy-4, 17 °C for FeCrAl and 22 °C for SiC. The difference between experimental data and Henry equation under the subcooled condition was 103 °C for Zircaloy-4, 181 °C for FeCrAl and 107 °C for SiC. Henry equation only considered thermal properties of specimens and liquid under the saturated condition without surface effect which also influenced on minimum film boiling temperature [11-16] was different from each specimen (Table 1). The minimum film boiling temperature of the experimental data and Henry equation were not identical. However, the tendency of the minimum film boiling temperature between the experimental data and Henry equation was identical (Zircaloy-4 > SiC > FeCrAl). Additionally, since surface would change due to oxidation during quenching, the material corrosion resistance would also influence on minimum film boiling temperature.

$$T_{MFB,H} = T_{MFB,B} + 0.42 \left\{ \left[ \frac{(\rho C_p k)_l^{0.5}}{(\rho C_p k)_s^{0.5}} \right] \left\{ h_{iv} / [C_{p,s}(T_{MFB,B} - T_{sat})] \right\}^{0.6} (T_{MFB,B} - T_i) \right\} \quad (2)$$

$$T_{MFB,B} = T_{sat} + 0.127 \left( \frac{\rho_v h_{iv}}{k_v} \right) \left[ \frac{g(\rho_l - \rho_v)}{(\rho_l + \rho_v)} \right]^{2/3} \left[ \frac{g(\rho_l - \rho_v)}{\sigma_{lv}} \right]^{1/2} \left[ \frac{g(\rho_l - \rho_v)}{\mu_v} \right]^{-1/3} \quad (3)$$

### 3. Conclusions

Quenching experiments were conducted with Zircaloy-4, FeCrAl and SiC under saturated and

subcooled condition. Cooling and heat flux curves were obtained. From cooling curve, the entire cooling time resulted from heat capacity of specimens in both the saturated and subcooled condition. From heat flux curves, minimum film boiling temperature and minimum heat flux were measured. The minimum film boiling temperature of experiments data as compared with the temperature calculated from equation of Henry. Since Henry did not consider surface effectiveness on minimum film boiling temperature, it was different from our results. However, the tendency of minimum film boiling temperature was identical to Henry's. For the future work, subcooled effect and surface effect on post-CHF parameters are worthy of further research.

### ACKNOWLEDGEMENTS

The work was supported by the National Research Foundation of South Korea (NRF) grant funded by the Korea government (MSIP) (NRF-2016K2A9A1A06925730).

### REFERENCE

- [1] Ragheb and Magdi. Fukushima Earthquake and Tsunami Station Blackout Accident. Summary paper, University of Illinois at Urbana-Champaign, 2011.
- [2] Rio Anshari and Zaki Su'ud, Preliminary Analysis of Loss-of-Coolant Accident in Fukushima Nuclear Accident, AIP Conference, 2012
- [3] S. Leistikow and G. Schanz, Oxidation kinetics and related phenomena of Zircaloy-4 fuel cladding exposed to high temperature steam and hydrogen-steam mixtures under PWR accident condition, Nuclear Engineering and Design 103 (1987) 65-84
- [4] Carmack, Jon, et al. Overview of the US DOE accident tolerant fuel development program. No. INL/CON-13-29288. Idaho National Laboratory (INL), 2013.
- [5] Pint, Bruce A., et al. "High temperature oxidation of fuel cladding candidate materials in steam-hydrogen environments." Journal of Nuclear Materials 440.1 (2013): 420-427.
- [6] YEOM, Hwasung, et al. Evolution of multilayered scale structures during high temperature oxidation of ZrSi<sub>2</sub>. Journal of Materials Research, 2016, 31.21: 3409-3419
- [7] ALI, Amir, et al. Survey of Thermal-Fluids Evaluation and Confirmatory Experimental Validation Requirements of Accident Tolerant Cladding Concepts with Focus on Boiling Heat Transfer Characteristics. Oak Ridge National Laboratory (ORNL), Oak Ridge, TN (United States), 2016.
- [8] Bromley, Leroy Alton. *Heat transfer in stable film boiling*. No. AECD-2295;(UCRL-122). 1948
- [9] Henry R.E. A correlation for the minimum film boiling temperature, chem. Eng. Prog. Symp. Series, no. 138, vol. 70, pp. 81-90, 1974
- [10] BERENSON, Paul Jerome. Film-boiling heat transfer from a horizontal surface. Journal of Heat Transfer, 1961, 83.3: 351-356.
- [11] Chinchole, A. S., P. P. Kulkarni, and A. K. Nayak. "Experimental investigation of quenching behavior of heated zircaloy rod in accidental condition of nuclear reactor with water and water based nanofluids." *Nanosystems: Physics, Chemistry, Mathematics* 7.3 (2016): 528.
- [12] Jo, HangJin, et al. "Boiling performance and material robustness of modified surfaces with multi scale structures for fuel cladding development." Nuclear Engineering and Design 291 (2015): 204-211.
- [13] Bromley, Leroy Alton. *Heat transfer in stable film boiling*. No. AECD-2295;(UCRL-122). 1948
- [14] Kang, Jun-young, et al. "Film boiling heat transfer on a completely wettable surface with atmospheric saturated distilled water quenching." International Journal of Heat and Mass Transfer 93 (2016): 67-74.
- [15] Kang, Jun-young, et al. "Minimum film-boiling quench temperature increase by CuO porous-microstructure coating." Applied Physics Letters 110.4 (2017): 043903.
- [16] Lee, Gi Cheol, et al. "Induced liquid-solid contact via micro/nano multiscale texture on a surface and its effect on the Leidenfrost temperature." Experimental Thermal and Fluid Science 84 (2017): 156-164.